

GeoFlow: European Microgravity Experiments on Thermal Convection in Rotating Spherical Shells under influence of Central Force Field

Th. von Larcher^{1,#}, B. Futterer², C. Egbers²,
R. Hollerbach³, P. Chossat⁴, P. Beltrame⁵, L. Tuckerman⁶, F. Feudel⁷

¹Institute for Mathematics, Free University Berlin, Germany, # larcher@math.fu-berlin.de

²BTU Cottbus, Dept. of Aerodynamics and Fluid Mechanics, Cottbus, Germany,

³Dept. of Applied Mathematics, University of Leeds, United Kingdom

⁴CNRS, Nice, France

⁵MPI for Physics of Complex Systems, Dresden, Germany

⁶PMMH-ESPCI, Paris, France

⁷Nonlinear Dynamics Group, University of Potsdam, Germany

Abstract

We report on the status of preparatory work in the GeoFlow Experiment which will take place on board Columbus Orbital Facility (*COF*) at the International Space Station (*ISS*). GeoFlow focus on investigations of the stability and dynamics of convective spherical gap flows under influence of a central force field. To exclude the unidirectional gravitational force which acts on earth's surface the planned long-time measurements have to take place in microgravity environment.

After a introduction and an overview of experiment hardware preparation status which includes application of measurement techniques, preparatory 3D numerical flow simulations as well as experimental work and the way of experiment data analysis are presented. Also some aspects of the experiment operation phase will be given. The paper is then closed with concluding remarks and an outlook on possible future GeoFlow reflight campaigns.

1. Introduction

Research on thermal convection in spherical gap flows is a suitable model in geophysical fluid dynamics. Instabilities provide details for understanding large scale geophysical flows as e.g. convective phenomena in Earth's outer core.

Yavorskaya et al. (1) discussed the fluid flow analogy of spherical gap flow model in atmospheric motion and convection in core regions of gaseous planets in theory. Microgravity research on convective flow stability in a spherical shell system was realised by Hart et al. who did experiments on board a NASA Space Shuttle in 1985 and in a reflight campaign in 1995 (cf. (2) and (3)). The experiment set-up consisted of a rotating hemispherical shell system with the possibility to apply a radial as well as a latitudinal temperature gradient, i.e. Equator-to-Pole temperature difference. Gravity was modelled by imposing a central electric field. The observed flow pattern was visualised by applying Schlieren technique and the experimental results were compared with 3D nonlinear simulations.

Use of central force fields as artificial gravity is in geophysical analogy regarding for example Earth's outer core as discussed by Früh (4) and also by Beltrame (5) who concluded that the essential character of the flow is captured even if the power law of artificial gravity due to central force field does not agree with acceleration due to gravity in earth.

The GeoFlow experiment focus on thermal-driven flows influenced by a central force field in a rotating full spherical gap model. Regarding fluid dynamics, the aim is to investigate the stability of flow states, pattern formation and transition to turbulence in viscous incompressible fluids. But research in spherical gap flows is also of interest in technical applications as understanding and controlling of such flows can be useful for e.g. pump systems, etc. As the central force field is realised by an electro-hydrodynamic force, in particular the dielectrophoretic effect, the study can also bring some new results in electro-viscous phenomena and in fluid transport applications.

To eliminate the unidirectional acceleration due to gravity on earth, these long-time experiments require microgravity environment. GeoFlow therefore is going to take place in the Fluid Science Laboratory (*FSL*) of Columbus Orbital Facility (*COF*). Launch of the GeoFlow Experiment Container and *COF* is scheduled to 6th December 2007. Experimental research can probably started in early January 2008 after commissioning of *COF* and *FSL*.

The overall preparatory research program comprises work packages as development of hard- and software as well as preparative experimental and numerical investigations. While experiments are performed using the Science Reference Model in the laboratory at BTU Cottbus and also in the laboratories of industrial

partners, the experiment hardware is built and verified by industry. Numerical investigations and bifurcation analysis are performed by European research groups from France, United Kingdom and Germany which are members of the GeoFlow Topical Team. These studies focus on preparation of the experiment design and on the observable parameter space by flow states simulations and on linear stability analysis and bifurcation analysis (cf. (6)-(12)).

2. Experiment Preparation

2.1 Experiment Set-up

The set-up consists of an inner sphere made of tungsten-carbide and two outer glass shells made of BK7-glass. In the research cavity a temperature difference is realised by heating the interior sphere and cooling the fluid in the outer gap between the outer glass shells using temperature-controlled fluid circuits filled also with silicone oil. The experiment cell is mounted on a rotating tray which allows for solid body rotation (cf. **Fig. 1** and **2**). A central force field which acts on the experiment fluid is generated by applying an alternating high voltage field, V_{rms} , between the interior sphere and the inner glass shell.

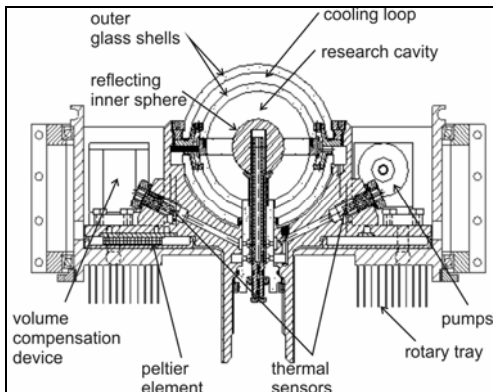


Fig. 1 Sketch of the experimental set-up.



Fig. 2 Science Reference Model.

A low viscosity silicone oil is used as working fluid. **Table 1c)** shows those physical properties which are most important for GeoFlow, measured at $T=25\text{ }^\circ\text{C}$, that is a good value for the average experiment environment temperature. In particular, in the expected environment temperature range which is approx. $20\text{-}35\text{ }^\circ\text{C}$, differences in physical properties from the given values are not significant enough to affect the fluid flow structures, e.g. $\rho(T=50\text{ }^\circ\text{C}) = 0.90\text{ g/cm}^3$ and $\rho(T=0\text{ }^\circ\text{C})=0.95\text{ g/cm}^3$. However, temperatures of the in- and outflow of the cooling and heating loop are measured regularly and possible effects on the flow structures will be considered in the data analysis.

While the Coulomb force does not affect the fluid due to high frequency alternation, the dielectrophoretic effect results in central force field and acts as ponderomotive force due to the geometrically inhomogenous electrical field. Table 1 shows geometric and dynamic parameters of the model as physical properties of the working fluid.

Regarding dimensionless parameters, the Taylor number Ta is proportional to the rotation rate Ω , $Ta \sim \Omega^2$. While in natural convection phenomena (i.e. in GeoFlow case $V_{\text{rms}}=0\text{ kV}$) the Rayleigh number Ra often denotes the temperature difference, in GeoFlow this parameter is called the central Rayleigh number Ra_{central}

Table 1 Experiment parameters

a) geometric dimensions of the research cavity

Inner radius r_i	13.5 mm
Outer radius r_o	27.0 mm
Gap width $r_i - r_o$	13.5 mm
Radius ratio $\eta = r_i / r_o$	0.5

b) variable experiment parameter

Rotation rate Ω	0-2 Hz
High voltage V_{rms}	0-10 kV
Temperature difference ΔT	0-10 K

c) physical properties of the working fluid

Type	Silicone oil
Density ρ	0.92 g/cm ³
Kinematic viscosity ν	$5 \cdot 10^{-6}\text{ m}^2/\text{s}$
Thermal conductivity λ	0.116 W/(K*m)
Thermal Diffusivity κ	$7.735 \cdot 10^{-8}\text{ m}^2/\text{s}$
Cubic exp coeff α	$108 \cdot 10^{-5}\text{ 1/K}$
Dielectric Constant ϵ_r	2.7
Therm. Coeff. of ϵ_r	$1.07 \cdot 10^{-3}\text{ 1/K}$

d) dimensionless parameters

Taylor number Ta	$Ta \leq 1.3 \cdot 10^7$
Central Rayleigh number Ra_{central}	$Ra_{\text{central}} \leq 1.4 \cdot 10^5$
Prandtl number Pr	$Pr = 64.64$

which is proportional not only to the temperature difference ΔT but also to the acceleration due to central force field, g_E , $Ra_{\text{central}} \sim (\Delta T * g_E)$. As g_E is proportional to $((V_{\text{rms}})^2 * r^{-5})$, it follows that $Ra_{\text{central}} \sim (\Delta T * (V_{\text{rms}})^2 * r^{-5})$. While acceleration due to gravity is approx. 10 m/s^2 on earth's surface, the largest value of acceleration due to high voltage field is approx. 10^{-1} m/s^2 at $r=r_o$, r_o as outer radius of the research cavity, and $V_{\text{rms}}=10 \text{ kV}$. Table 1d) shows values of Ta and Ra_{central} , resp. The Prandtl number Pr reflects physical properties of the working fluid, $Pr=v/\kappa$. The Rayleigh number Ra is used here only when natural convection phenomena are investigated in preparatory work.

2.2 Measurement techniques

In a first experimental and numerical study, funded by ESA, we found common tracer particles to be in principal suitable for quantitative flow field measurements under the given experiment conditions, e.g. using Laser Doppler Velocimetry. Here, the high voltage field was defined to be the most critical parameter as it has the potential to deflect the movement of the particles relative to the fluid flow field which would then have an influence on those measurements. Several additional tests, e.g. due to crew safety, are necessary to make these particles acceptable for space research and to perform particle laden fluid flow experiments in future GeoFlow campaigns.

In the first campaign, measurements of the flow field are therefore done using the Wollaston-Shearing-Interferometry (WSI). Schlieren technique and Shadowgraphy is implemented within FSL and can be an option for GeoFlow. Due to Experiment constraints, measurement techniques are used in reflection mode. The inner sphere of the set-up is prepared to act as a mirror. **Fig. 3** shows a sketch of the WSI set-up at BTU laboratory used for preparatory experimental works. Because of the acceleration due to gravity, the operation mode on earth is parallel to the axis of the gravitational force (g).

The Adaption Optics (AO) includes an optical lens tool which converts the planar waves emitted by the Laser (Q) into spherical waves and the reflected waves vice versa. This is needed due to the spherical geometry of the experiment shell system. The 90° mirror (US) deflects the beams to the AO which focus the waves to the center of the experiment cell (EM). The beam separation cube (ST) deflects the reflected beams, coming from the AO, to the Wollaston Prism (W) and the Polariser (PO). Details of the functionality of these items can be found in the standard literature.

The WSI method principally detects refractive index gradients and is therefore sensitive to density gradients caused by temperature differences in the GeoFlow experiment. Optical path length variations results in interference phenomena which are directly photographed by a CCD camera (K). **Fig. 4** shows WSI images from ground test sequences at industrial lab taken at different parameter points. Note the

complicated interferogram structures at large Taylor numbers.

The interferogram pattern could be affected by distortions caused by the spherical shell set-up and effects of the optical items, particularly substantial in the marginal areas of the experiment cell. Of course, such effects are considered in the image processing. However, their significance is under discussion yet.

Since the WSI delivers images of interference pattern, the goal of the WSI data analysis is to get informations about the temperature field, that corresponds to the flow field, and its time-dependent behaviour. This is part of the experimental and numerical preparatory work within GeoFlow which is discussed below.

2.3 Preparatory 3D numerical flow simulations

Numerical simulations using a pseudospectral method by Hollerbach (13) including linear stability

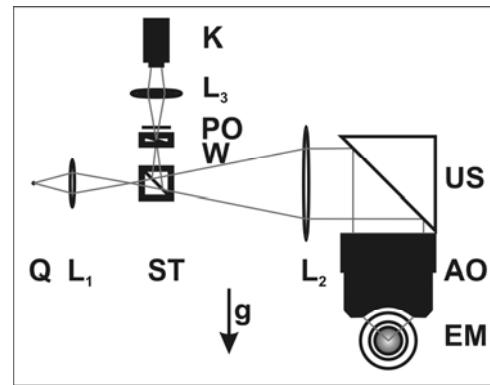


Fig. 3 Sketch of the WSI set-up at BTU-Laboratory. Q=Laser, L=Lens, ST=Beam Separation, US= 90° mirror, AO=Adaption Optics, EM=Science Reference Model, W=Wollaston prism, PO=Polarisator, K=CCD Camera, g =gravity vector.

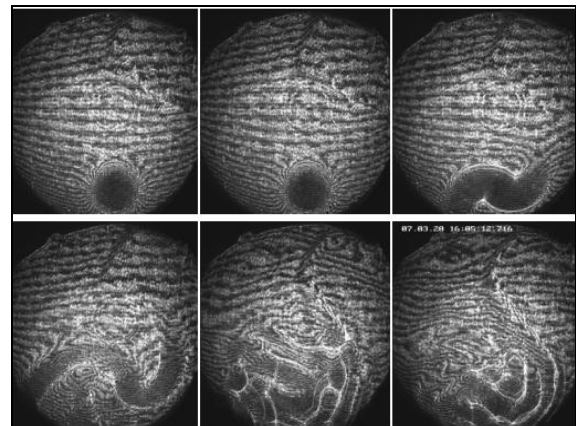


Fig. 4 Natural Convection ($V_{\text{rms}}=0 \text{ kV}$). WSI images taken at constant Rayleigh number $Ra=4.31*10^6$ and different Taylor numbers. From top left to down right: $Ta=0$, $Ta=8.6*10^2$, $Ta=1.3*10^5$, $Ta=5.4*10^5$, $Ta=1.1*10^7$, $Ta=1.3*10^7$.

analysis are performed in the experiment preparation phase to design the experimental set-up, in particular the geometric parameters of the gap, and to predict the experiment scenario. **Fig. 5** shows an overview of numerical solutions of flow states which occur by varying Ra and Ta , resp. The solid line is calculated by linear stability analysis, the dashed line denotes the transition from time-dependent stable solutions to irregular flows. In addition, regions of most stable mode m are shown. As the $Ra=5000$ line shows, superposition of rotation can make an irregular flow steady convective. That is also confirmed by numerical simulations (cf. **Fig. 6**).

A special focus in the 3D simulation is on the calculation of flow states including flow field and temperature field at selected parameter points of the defined experiment flow plan to support the experimental data analysis (cf. **Fig. 7**).

Furthermore, construction of artificial interferograms from the calculated temperature fields is necessary for evaluation and interpretation of experiment data (see below).

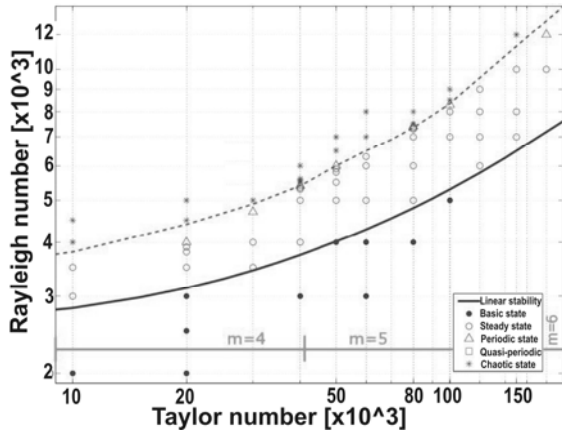


Fig. 5 Stability diagram calculated from numerical simulations (cf. (6)).

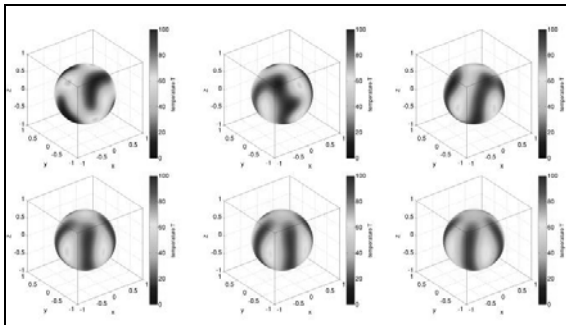


Fig. 6 Temperature field visualized on spherical surface in the gap, scaled to 100%, calculated for $Ra_{\text{central}}=5000$ and different Taylor numbers. From top left to down right: $Ta=1 \cdot 10^4$, $Ta=2 \cdot 10^4$ (both irregular flow), $Ta=4 \cdot 10^4$ (periodic flow state), $Ta=6 \cdot 10^4$, $Ta=8 \cdot 10^4$, $Ta=1 \cdot 10^5$ (all steady flow).

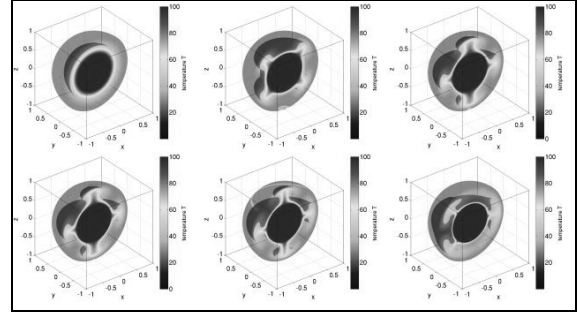


Fig. 7 Temperature field visualized in hemispherical shells, scaled to 100%, calculated for $\eta=0.5$, $Pr=64.64$, $Ta=0$ and different central Rayleigh number. From top left to down right: $Ra_{\text{central}}=2 \cdot 10^3$ (conductive state), $Ra_{\text{central}}=5 \cdot 10^3$, $Ra_{\text{central}}=8 \cdot 10^3$, $Ra_{\text{central}}=1 \cdot 10^4$, $Ra_{\text{central}}=2 \cdot 10^4$ (all steady axisymmetric flow states), $Ra_{\text{central}}=5 \cdot 10^4$ (time dependent (irregular)).

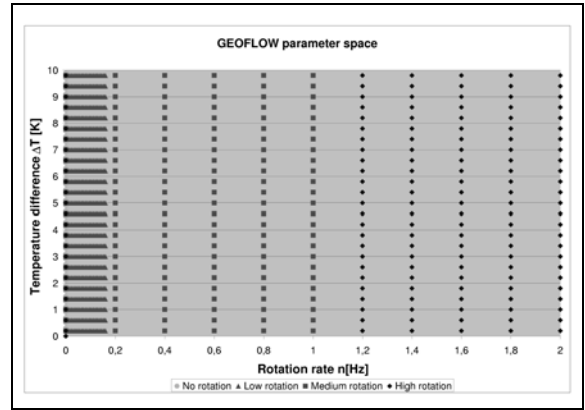


Fig. 8 Sketch of high resolution parameter scan. Symbols are explained within the figure.

3 Experiment Operation

3.1 Experiment Flow Plan

The developed experiment flow plan based in part on numerical predictions in other parts on experiences by the science teams. Since the high voltage will be set-up to a constant value of 10 kV, free parameters are the temperature difference (Ra_{central}) and the rotation rate (Ta). The expected experiment duration time of several weeks allows for a high resolution parameter scan (cf. **Fig. 8**).

To investigate the dependence of solutions on initial conditions, i.e. flow patterns at given parameter values, some experiment sequences started e.g. with a sudden temperature difference while others increase ΔT smoothly. Main part of the first experiment run is the investigation of flow patterns at rotation rate 0, i.e. varying only the temperature difference without rotation. After this, superposition of rotation will be set-up.

3.2 Data analysis

A quantitative analysis of the experiment data will need the support of numerical simulations. **Fig. 9** shows the way of data processing and evaluation and interpretation, resp. The simulation of 3D temperature fields which are then used for construction of artificial interferograms (forward modelling,

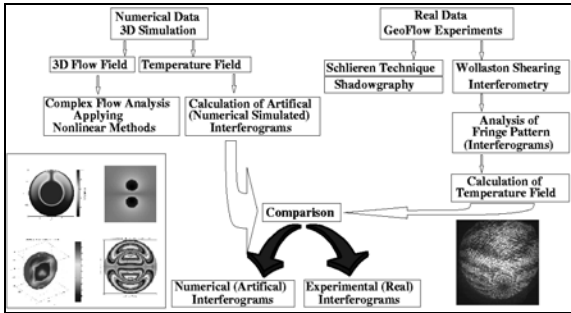


Fig. 9 Numerical and experimental data analysis. Verification of experimental data by analysis and comparison with numerical data.

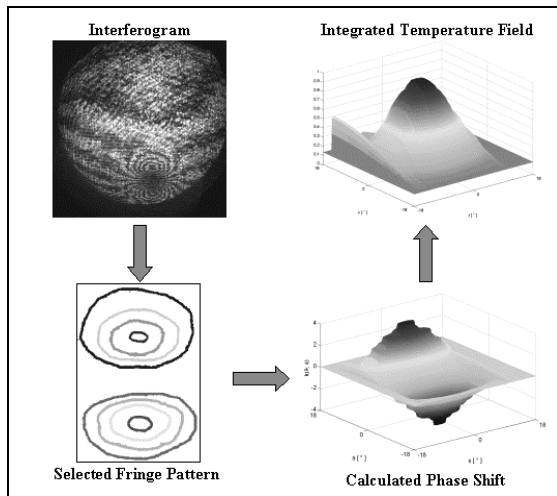


Fig. 10 Work Flow for interferogram evaluation of experimental data (inverse modelling).

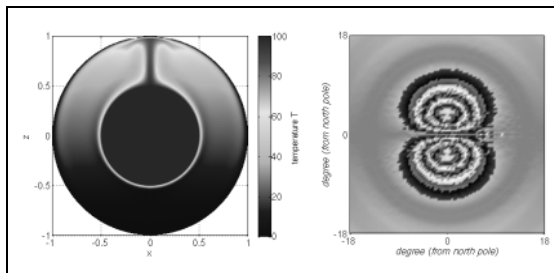


Fig. 11 Forward Modelling. Parameters: $Ra=8.09 \cdot 10^6$, $Ta=0$ ($\Delta T=15.0$ K, $\Omega=0$ Hz, $V_{rms}=0$ kV).

left hand side) allows for a comparison with experimental interferograms. On the other hand, calculation of integrated 2D temperature fields based on experimental interferogram data (inverse modelling, right hand side) allows for comparison with numerical calculated temperature fields. By using both data sets in a useful manner, the observed flow pattern can be analysed in detail. Also the numerical simulations can be verified with experimental data.

In addition, applying linear and nonlinear time series analysis methods on numerical flow field data, i.e. using

the calculated kinetic energy or the nusselt number, allows for a characterization of the flow dynamics. In particular, dynamic variables as, e.g., Lyapunov exponents, and a dimension analysis of the (reconstructed) phase space, will be calculated to analyse the complexity of the numerical simulated flow pattern.

Putting the results of the numerical and experiment data analysis together allows for a detailed characterization of the observed flow states.

The analysis procedures are realised by the scientific teams and the two ways of data analysis are tested successfully, especially the inverse modelling method is verified by using ground test data which are measured in scientific test campaigns. As an example for inverse modelling, **Fig. 10** shows the work flow for a given experimental interferogram taken at a temperature difference of $\Delta T=4$ K.

Fig. 11 shows an example for forward modelling. The calculated flow pattern is a steady state in case of natural convection, i.e. $V_{rms}=0$ kV.

Summary

We presented an overview of the status of experimental and numerical preparatory work and the way of data analysis within the GeoFlow project.

The experiment flow plan, that is developed with the support of linear stability analysis as well as on basis of 3D numerical simulations which confirm the stability analysis, allows for high resolution parameter scan.

The experiment data will be analysed using mathematical tools and also by comparing numerical simulations which are extended to calculation of artificial interferograms.

Recent NASA/ESA project status is to launch the Columbus Orbital Facility on 6th December 2007 with NASA Space Shuttle 'Atlantis'. On board this flight the GeoFlow experiment container will be brought to ISS too. After commissioning of COF and the Fluid Science Laboratory (FSL) where GeoFlow will take place the experiment can be started, that is scheduled to early January 2008.

Outlook

While the first GeoFlow campaign will probably be done in the first months of 2008, reflight campaigns are under discussion yet. Here, possible scenarios are a) variation of experiment fluid's viscosity since higher viscous fluid motion would lead the physical model to mantle convection, b) variation of gap width as a narrower spherical gap would lead to Earth atmosphere conditions and c) change of geometry, i.e. use of a cylindrical gap instead of a spherical one, so that technical applications can be explored.

Acknowledgement

The GeoFlow project is funded by ESA (grant no. AO-99-049) and by German Aerospace Center DLR

(grant no. 50 WM 0122). The authors would also like to thank ESA for funding the GeoFlow Topical Team (grant no. 18950/05/NL/VJ). The scientists also thank the industry involved for support, namely Astrium GmbH, Friedrichshafen, Germany and the User Support Center MARS, Naples, Italy and E-USOC, Madrid, Spain.

References

- 1) Yavorskaya, I.M., Fomina, N.I. and Belyaev, Y.N., *Acta Astronautica* **11**, 1984
- 2) Hart, J.E., Glatzmeier, G.G. and Toomre, J., *J. Fluid Mech.* **173**, 1986
- 3) Hart, J.E. et al., *NASA-TP-1999-209-576*, 1999
- 4) Früh, W.-G., *Nonlin. Proc. in Geophys.*, **12**, 2005
- 5) Beltrame, P., Travnikov, V., Gellert, M. and Egbers, Ch., *Nonlin. Proc. in Geophys.*, **13**, 2006
- 6) Gellert, M., Beltrame, P. and Egbers, Ch., *Journal of Physics: Conference Series*, **14**, 2005
- 7) Futterer, B., Gellert, M., von Larcher, Th. and Egbers, C., *Acta Astronautica*, **62**, 2008
- 8) Beltrame, P. and Egbers, C., *Proc. Appl. Math. Mech.*, **4**, 2004
- 9) Beltrame, P., Egbers, C. and Hollerbach, R., *Advances in Space Research*, **32**, 2003
- 10) Travnikov, V., Egbers, C. and Hollerbach, R., *Advances in Space Research*, **32**, 2003
- 11) Egbers, C., Beyer, W., Bonhage, A., Hollerbach, R. and Beltrame, P., *Advances in Space Research*, **32**, 2003
- 12) Futterer, B., Brucks, A., Hollerbach, R. and Egbers, Ch., *Int. J. Heat Mass Transfer*, **50** 2007
- 13) Hollerbach, R., *Int. J. Numer. Meth. Fluids*, **32**, 2000